The Journal of Experimental Biology 214, 915-920

doi:10.1242/jeb.051128

RESEARCH ARTICLE

Non-wetting wings and legs of the cranefly aided by fine structures of the cuticle

Hsuan-Ming S. Hu[1], Gregory S. Watson[1], Bronwen W. Cribb[2] and Jolanta A. Watson[1,*]

[1]School of Pharmacy and Molecular Sciences, James Cook University, Townsville, QLD 4811, Australia and [2]Centre for Microscopy and Microanalysis and School of Integrative Biology, University of Queensland, St Lucia, QLD 4072, Australia

*Author for correspondence (jolanta.watson@jcu.edu.au)

Accepted 24 November 2010

SUMMARY

Non-wetting surfaces are imperative to the survival of terrestrial and semi-aquatic insects as they afford resistance to wetting by rain and other liquid surfaces that insects may encounter. Thus, there is an evolutionary pay-off for these insects to adopt hydrophobic technologies, especially on contacting surfaces such as legs and wings. The cranefly is a weak flier, with many species typically found in wet/moist environments where they lay eggs. Water droplets placed on this insect's wings will spontaneously roll off the surface. In addition, the insect can stand on water bodies without its legs penetrating the water surface. The legs and wings of this insect possess thousands of tiny hairs with intricate surface topographies comprising a series of ridges running longitudinally along the long axis of the hair fibre. Here we demonstrate that this fine hair structure enhances the ability of the hairs to resist penetration into water bodies.

Supplementary material available online at http://jeb.biologists.org/cgi/content/full/214/6/915/DC1

Key words: wing, leg, insect, anti-wetting, atomic force microscopy, hair, water, adhesion.

INTRODUCTION

The wettability of surfaces is a fundamental property that has attracted great interest and been the subject of many studies (Adamson, 1990; de Gennes, 1985; Fowkes, 1964; Holloway, 1970). One of the driving forces for a more detailed understanding of the phenomenon has been the need to design new materials with specific and tailored surface properties. For example, a superhydrophilic surface with a contact angle (CA) of almost 0 deg has been successfully used as a transparent coating with anti-fogging and self-cleaning properties (Wang et al., 1997). In addition, many hydrophobic surfaces have been shown to inhibit contamination, adherence to snow, erosion and even electrical conductivity (Lafuma and Quere, 2003; Sun et al., 2005).

Interesting wetting properties have been observed on many naturally occurring patterned surfaces (Bhushan and Jung, 2008; Burton and Bhushan, 2005; Chiou et al., 2007; Lau et al., 2003; Ma and Hill, 2006; Martines et al., 2005; Nosonovsky and Bhushan, 2007; Nosonovsky and Bhushan, 2008; Parker and Lawrence, 2001; Zhang and Low, 2007). Indeed, nature has provided us with an immense and relatively untapped reservoir of micro- and nano-structuring exhibiting finely tuned functional efficiencies. The water contact angles of insect surfaces show a wide variation that is broadly correlated with surface roughness and with habitat. Holdgate has characterized four major groups of insects in relation to their water wetting properties (Holdgate, 1955). One of the more interesting groups is terrestrial and aquatic species whose surfaces are very rough or covered with hair piles. They have very high advancing and receding CAs, often over 150 deg, which generally indicates low adhesion to water. These adaptations are more often than not structural rather than chemical as many insects already have a chemistry that is near the upper limit for smooth surfaces. Hair piles on terrestrial insects may help them to contend with the risks associated with living in an environment that offers little protection against wetting by rain and other water surfaces which the insect may encounter (Watson et al., 2010b; Watson et al., 2010c). As with other insect cuticular structures, hairs may have multiple purposes such as aiding in flight (contributing to aerodynamic factors) (Perez-Goodwyn, 2009).

Many of these insect fine structures increase the surface roughness of the cuticle. There are a number of theories to express the surface wettability based on surface roughness, all of which have certain assumptions and limitations. Cassie and Baxter express the wetting state in terms of a number of interfaces: a liquid–air interface with the ambient environment surrounding the droplet, and a surface under the droplet involving solid–air, solid–liquid and liquid–air interfaces (Cassie and Baxter, 1944). Eqn 1 shows the CA formed with a rough surface (θ_C):

$$\cos\theta_C = R_f f_{SL}\cos\theta + f_{SL} - 1 , \quad (1)$$

where R_f is the roughness factor defined by the solid–liquid area to its projection on a flat plane (the roughness factor of the wetted area), f_{SL} is the fraction of the solid–water interface (the area fraction of the projected wet area), and θ represents the CA that would occur on a smooth surface of the identical chemistry and can be expressed by Young's relation $\theta=\cos-1[(\gamma_{SV}-\gamma_{SL})/\gamma_{LV}]$ where the γ_{ij} terms correspond to the solid–vapour, solid–liquid and liquid–vapour interfacial energies/tensions.

One of the many insects that demonstrate a hierarchy of surface roughness is the cranefly: one of the most abundant species of all the Diptera. As the craneflies are notable lovers of moisture, they inhabit a diverse range of habitats where water is available, and are typically found resting on foliage overhanging water sources in damp shady locations. The larvae mainly emerge from water or semi-liquid matter (e.g. mud) to become adults and most species cease to feed

after this stage. The adults exhibit a slender body and extremely long legs, with wings spanning 8–75 mm and characterized by having two anal veins reaching the margin. The adults fly slowly and irregularly close to moist grounds with their legs making regular contact with the substrate.

As the cranefly has exceptionally long legs and is often found in damp environments, the insect will be susceptible to detrimental adhesional contacts, as well as breakage in the worst-case scenario. The insect can potentially become a victim of permanent immobilization on water or wetted surfaces with a reduced capacity to evade or fight off predators. In this paper we demonstrate how the fine structure of cranefly (*Nephrotoma australasiae*) hairs on the legs enhances their ability to repel water. Smaller hairs found on the wings have a similar structure and we show that this architecture also aids the insect under rain/droplet conditions.

MATERIALS AND METHODS

Photography

A Canon Digital 350D SLR and a Canon Ultrasonic EF-S 60 mm macro-lens were used to obtain 8 megapixel resolution photographs. Cropping, adjustment of brightness and contrast, and scale bar addition were carried out using Photoshop 7.0.

Optical microscopy

An AIS optical microscope VG8 (Australian Instrument Services, Croydon, Victoria, Australia) attached to a Panasonic colour CCTV camera WV-CP410/G as well as an XSP series compound microscope (York Instruments, Sydney, NSW, Australia) were used. These were placed in a vertical, horizontal or inverted position to obtain top, side and bottom views, respectively. Magnifications of up to ×40 were used.

Scanning electron microscopy

Individual hairs were attached to atomic force microscope (AFM) probes and wing/leg tissues (wing approximately 3 mm×3 mm, leg approximately 1 mm) were held on an aluminium pin-type stub with carbon-impregnated double-sided adhesive. Samples were sputter coated with 7–10 nm of platinum prior to imaging with a JEOL 6300 field emission scanning electron microscope (SEM) at 8 kV.

Atomic force microscopy

Force measurements including hair mechanical properties and adhesion data were obtained by a TopoMetrix (Veeco Instruments, Plainview, NY, USA) Explorer TMX-2000 scanning probe microscope (SPM) with a $130\times130\,\mu m^2$ tripod scanner that has a z-range of 9.7 µm. Operated under ambient air conditions (temperature of 22–23°C and 60–75% relative humidity, RH) and using force *versus* distance (F–d) mode, F–d curves consisting of 600 data points were acquired at rates of translation in the range 2–5 $\mu m\,s^{-1}$ in the z-direction. Calibration along the z-direction was carried out according to previous studies (Watson et al., 2004b; Watson et al., 2002).

Five 'beam-shaped' tipless levers (NT-MDT Ultrasharp, Moscow, Russia) with stiffness constants (k_N) determined by accepted methods (Cleveland et al., 1993) were used on 10 individual uncoated cranefly hairs. Twenty F–d curves were obtained for both the force constant and the adhesion measurements; hairs were then thin and thick coated with polydimethylsiloxane (PDMS; Sylgard-184, Dow Corning, Corning, NY, USA) and new values were obtained after each coating had dried (24 h). Stiffness of the hairs was obtained using methods described previously (Gibson et al., 1996). Adhesion data between a hair attached to the lever and a 10 µl droplet of Milli-Q water were obtained with the droplet deposited on a slide previously coated with PDMS to ensure a hydrophobic substrate. The hair was brought into contact roughly 500 µm below the top of the droplet (supplementary material Fig. S1) in order to avoid the meniscus attraction between the hydrophilic lever and the Milli-Q water.

Hair attachment and coating

Cranes flies (*N. australasiae*, Skuse 1890) were captured in the Brisbane and Townsville areas of Queensland, Australia, in close proximity to waterways. The longest cranefly hairs (see Results and Discussion) were scraped off the legs using a surgical scalpel and glued to the end of tipless levers under an optical microscope. The lever was attached to an in-house x-, y- and z-positioning translator. This arrangement allowed the small, micrometre-sized particles/bodies to be attached to the lever (Watson et al., 2004a). The free end of the lever was lowered onto the edge of a glue droplet (fast-curing two-part epoxy resin) and then onto the end of the desired hair base followed by drying for 24 h. Force measurements of the hair spring constant required the hair base to remain fixed by its attachment to AFM non-compliant chips.

Polymer coating was conducted under an optical microscope. A droplet of PDMS (10:1 base to curing agent mixture) was deposited onto a concave microscope slide and allowed to spread for *ca*. 1 min. A thin PDMS coating was achieved by positioning the lever with a cranefly leg hair attached to the free end at the

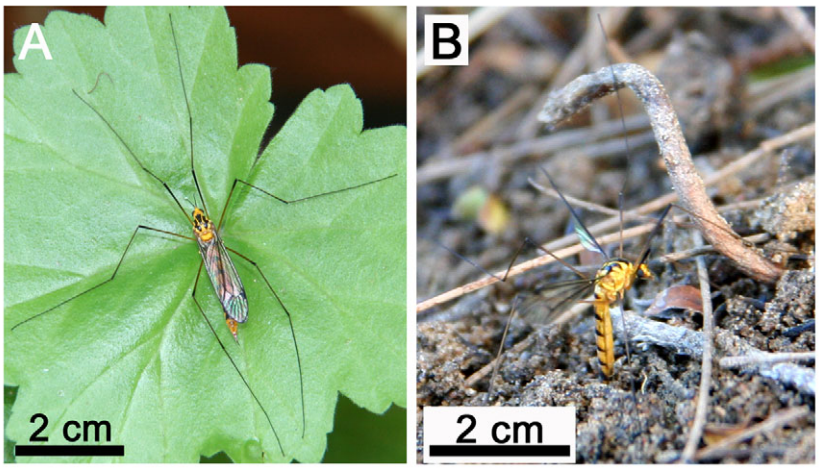

Fig. 1. (A) Resting cranefly (*Nephrotoma australasiae*) with a large contact area with the underlying leaf as a result of their extremely long legs. (B) An ovipositing cranefly at the bottom of the up–down flying pattern on moist/muddy soil showing the legs and the tip of the abdomen in contact with the underlying substrate.

edge of the PDMS droplet and gently lowering it, ensuring full coverage of the hair, but not of the lever itself. The hair was then slowly retracted and allowed to cure for a minimum of 48 h under ambient conditions prior to any further experimentation. This resulted in the hair having a thin coating of PDMS (thickness range 50–150 nm) whereby only the nanometer-sized structures were coated, leaving the main channels intact (supplementary material Fig. S2A). A thick PDMS coating was achieved by initially partially curing the deposited PDMS mixture on the slide at 60°C for 3 min before cooling it back to room temperature prior to dipping the hair. This resulted in a slightly thicker consistency of the PDMS, ensuring full coverage of the hair shaft channels as seen in supplementary material Fig. S2B. The free end of the hair was then gently lowered to the edge of the PDMS droplet (five times in succession for a thick coat) with the fully covered hair then cured for *ca*. 48 h under ambient conditions prior to experimentation.

RESULTS AND DISCUSSION

A photograph of the cranefly (*N. australasiae*) studied here is shown in Fig. 1. The cranefly at rest demonstrates a large contact area with the underlying substrate, e.g. leaves and wet soil, because of the extremely long length of the legs.

Some of the specimens used in this study were collected along the edges of a freshwater river. Observation of the flying habits of these insects (12 insects in total) showed a bouncing motion across the substrate (leaf litter, moist muddy soil and water surfaces). This bouncing comprised a near-vertical ascent of 3–8 cm and then a downward motion in which the insect legs came into contact with the ground and water surfaces. The duration of the up–down cycle was typically around 0.3 s (3.3 Hz). The observed flying behaviour is demonstrated by ovipositing craneflies where the tip of their abdomen frequently contacts the substrate (White, 1951) (Fig. 1B). The impact force of the legs with the ground appeared to be relatively large and this led us to speculate that the long legs are used as springs to control the impact with the ground and/or possibly help propel the insect on the vertical ascent part of the cycle. As the flying motion necessitates leg contact with moist ground it would seem advantageous for the leg to feature structural patterning to aid in repelling water.

Interaction of the cranefly leg and wing with water of various length scales (rain drops, ponds, rivers, etc.) is shown in Fig. 2. The hair piles in all circumstances resulted in an initial contact in which the droplets attained a near-spherical shape. The water droplet exhibited a CA of over 170 deg with the wing as shown in Fig. 2A. The apparent CA of a water droplet supported by a syringe tip and placed on the cranefly leg was also extremely high (Fig. 2B). Micro-droplets from a mist spray exhibited similar CAs on both wing and leg surfaces. Fig. 2C–E shows droplets being held up by hairs on the wing vein, wing membrane and leg, respectively. The images

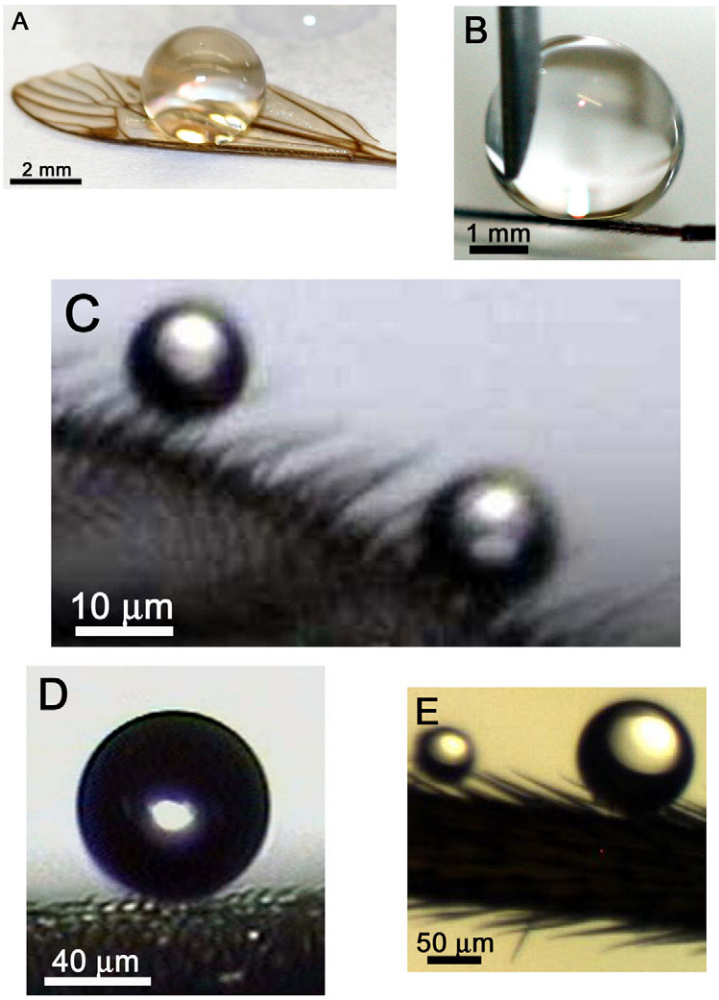

Fig. 2. Optical images showing a 10 µl water droplet displaying superhydrophobic contact on a cranefly wing (A) and leg with the water droplet supported by a syringe to avoid roll off (B). Micro-droplets of water from a mist sprayer were supported by hairs on the wing veins (C), wing membrane (D) and leg (E).

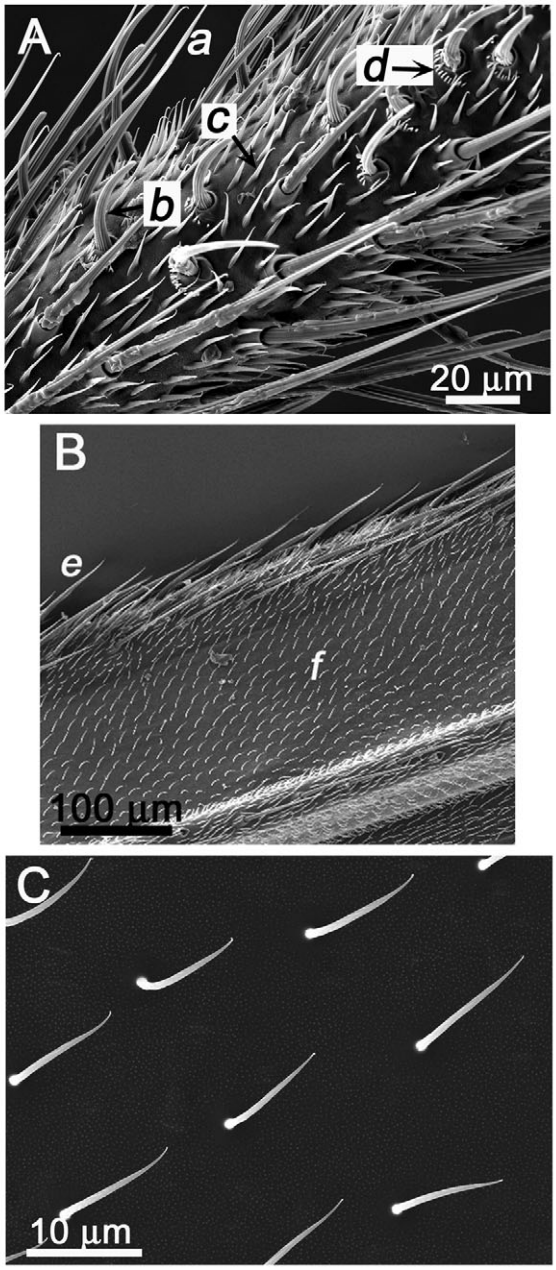

Fig. 3. (A) Scanning electron microscope (SEM) images of a cranefly leg with four different types of hair (types ‘a’, ‘b’, ‘c’, ‘d’) with nanogrooves visible on hair types ‘a’, ‘b’ and ‘c’. (B) SEM images of different sized hairs (types ‘e’ and ‘f’) on a cranefly wing (with longer type ‘e’ hairs on the wing edge and the veins). (C) High magnification SEM image of a cranefly wing showing type ‘f’ hairs.

demonstrate the apparent superhydrophobic nature of the cuticles, causing water droplets to spontaneously roll off the cuticle surface.

An SEM image of a small region along the cranefly leg is shown in Fig. 3A where four types of hair exist (types ‘a’, ‘b’, ‘c’ and ‘d’). Hair type ‘a’, the most protruding hair, is 90±15 µm in length and angled at 25±5 deg to the inner leg shaft surface. This tilt arrangement is similar to that of the hairs observed on water striders, which need to maintain function above the surface of the water (Watson et al., 2010a). However the length and width of the type ‘a’ hairs on the cranefly are typically three times greater than those reported on striders (Watson et al., 2010a).

A low magnification SEM image (Fig. 3B) shows the majority of the wing is covered in a uniform array of small hairs (type ‘f’) where the mean length and spacing of the hairs on the membrane are 12±1.5 µm and 14±2 µm, respectively (Fig. 3C). The larger hairs (type ‘e’), found on the wing veins, are comparable to the longest hair type ‘a’ on the legs.

The finer structures of cranefly hairs are shown in Fig. 4. Small type ‘e’ hairs on the wing (Fig. 4A) have arrow-like grooves that are similar in appearance to the hairs found on water strider legs (Watson et al., 2010a). Type ‘a’ hairs on the legs (Fig. 4B) have a micro-/nano-architecture consisting of a number of ridges (around 500 nm deep) running along the hair shaft while ultrafine channels run diagonally and meet at the apex and base of the large grooves.

Fig. 5A shows a cranefly leg floating on water with the hairs on the side of the leg dimpling the surface (highlighted by the arrows). To investigate whether the architecture (i.e. the grooves) aids in a hair’s ability to resist water penetration, individual type ‘a’ hairs were coated with the hydrophobic polymer PDMS (CA ~101 deg) (Watson et al., 2008) to maintain the chemical contribution to the process. The interaction of individual hairs (uncoated and coated) with water droplets is shown in Fig. 5B–D. Uncoated hairs attached to AFM cantilevers were brought into contact with a water droplet with loading forces of up to 1.26 µN and were unable to penetrate the water surface. Fig. 5B shows the dimple on the droplet surface between points *i* and *ii* created by the contacting uncoated hair. However, the water surface became penetrable when effects from both types of groove structure were removed by a thick PDMS coating (Fig. 5D). A thinner coat of PDMS completely covering the hair surface without filling the deeper grooves also prevented the hair from penetrating the water surface (Fig. 5C).

AFM adhesion measurements were carried out on uncoated and coated hairs interacting with water. The results showed that uncoated and thinly coated hairs yielded similar adhesion values (17.9±4.3 and 35.6±6.2 nN, respectively) suggesting that the deeper grooves were still prominent with a thin coating (supplementary material Fig. S2B). The adhesion of the thickly coated hair (the width of which was still similar to that of the uncoated hair; supplementary material Fig. S2) with water became more than 10 times greater

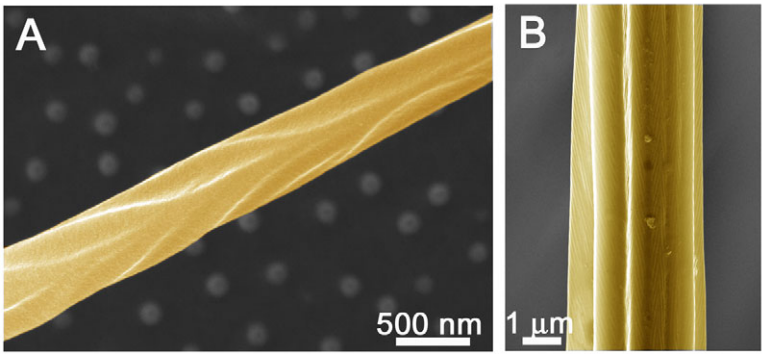

Fig. 4. SEM image of the fine surface structure found on a small wing hair (A) and a leg hair (B), which show grooves with ultrafine channels at about 45 deg that meet at the top and bottom of the larger grooves.

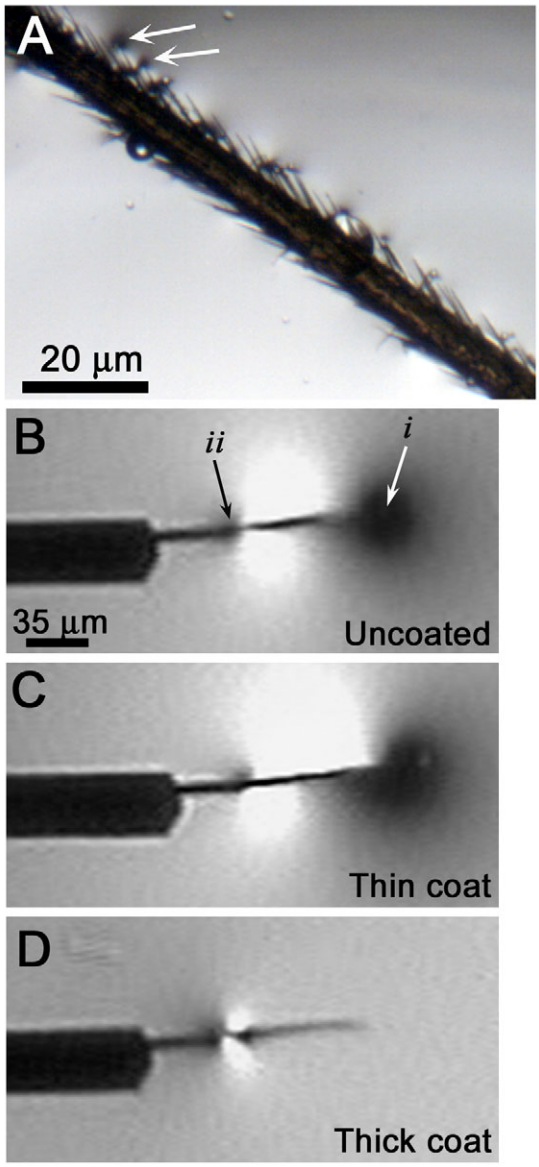

Fig. 5. (A) Optical image showing cranefly hairs on the side of the leg dimpling the water surface (indicated by arrows). (B–D) Optical images showing the interaction of individual cranefly hairs (type 'a') with water. (B) An uncoated hair not penetrating the water surface as observed by the formation of a dimple on the droplet surface from points *i* to *ii*. (C) A hair thinly coated with the hydrophobic polymer PDMS also dimpling the water surface. (D) A thickly coated hair penetrating the droplet surface.

without the surface structures (in excess of 500 nN), highlighting the significant role of the hairs' nano-roughness in both reducing adhesion and resisting water penetration.

The results from the interaction of individually coated and uncoated hairs with droplets sheds light on the importance of the micro-/nano-structuring in repelling water from the wing surface. The hairs that were covered with a thin coating of PDMS still retained a significant amount of the topographical structure (troughs) as shown in the SEM images (supplementary material Fig. S2A). These thinly coated hairs, like the uncoated hairs, did not penetrate the water surface under load. Thickly coated hairs, where the topographical structure components were reduced or completely removed (supplementary material Fig. S2C) resulting in a much smoother coating, did, however, penetrate the water surface. Moreover, the spring constants of the coated hairs did not alter enough to account for hair penetration. This indicates that the micro-/nano-roughness consisting of the open architecture of ridges with troughs is responsible for this effect as the chemistry is maintained (for thin and thick coats) and only the topographical component is altered. The much finer grooves did not appear to significantly contribute to the resistance to water penetration as these were removed by a thin coating. The higher adhesion values measured on thickly coated hairs in comparison to thinly coated samples also support findings that the larger groove structure is the important feature in minimizing contact with the water body.

An ideal architecturally enhanced non-wetting surface has the maximum ability to withstand water intrusion while allowing the liquid to have maximum mobility on the surface (high CA with low CA hysteresis). However, a trade off exists between enhancing the two properties when using only one layer of architecture (Bush et al., 2007; Extrand, 2006).

In order to maintain high hydrophobicity and buoyancy, air needs to remain within the asperities underneath the liquid body. Dense asperities are less likely to be penetrated by water and are found on the legs of fast swimmers like the water strider (Bush et al., 2007). The legs have a high f_{SL} that pins the solid–liquid–air contact line, requiring high pressure to drive out the air.

Unlike water striders (Wei et al., 2009), craneflies do not experience high hydrodynamic pressure from their leg strokes and thus may not require a dense type 'a' hair layer (Lafuma and Quere, 2003). It may be desirable for the most protruding hair layer (type 'a') of the cranefly legs to be less dense (up to 10 times more sparse) than that of water strider legs to increase droplet mobility. Longer (~3 times) and more rigid hairs (spring constant twice as high) are also more desirable in order to resist surface tension drawing the hairs together (Perez-Goodwyn, 2009).

Despite cranefly leg hairs being longer and thicker, their adhesion is similar to that of the water strider (Watson et al., 2010a); both being greatly reduced by their surface grooves. The micro-grooves not only contain more air to increase buoyancy and hydrophobicity but also reduce the adhesion to water and to other undesirable surfaces, as well as providing structural rigidity without the additional weight and material.

The four types of hair with different structure and dimensions may play different roles in insect functioning. Many insects have multiple layers of features on their cuticles that combine to prevent wetting by water bodies of different length scales (Andersen and Cheng, 2005; Watson et al., 2010b; Watson et al., 2008). As shown in Fig. 2E, it is the long hairs (type 'a') on the legs that will first come into contact with water bodies as they extend beyond the smaller hair piles. Loading pressure from a large water body causes the taller hairs to collapse towards the shorter hair layers until the loading force is balanced by the combined stiffness from all the contacting hairs. The thick shorter hairs have a curvature that aligns the top half of the hair with the free surface, forming a more efficient air trap (Cheng, 1973). The multi-layer hair is a feature in other semi-aquatic insects where an air plastron for submergence is required (Perez-Goodwyn, 2009). Type 'c' and 'd' hairs may also contribute to functions other than anti-wetting because of the small hair lengths (e.g. sensory) (Perez-Goodwyn, 2009).

Small water droplets that fall between the long hairs (types 'a' and 'b') can be prevented from contacting the underlying membrane by the shorter hairs beneath (types 'c' and 'd'). The mobility of droplets (mist or other smaller droplets) generally increases as they coalesce, with a corresponding increase in mass. Some smaller

droplets may also become absorbed by larger droplets from above, which will then roll off (Watson et al., 2010b; Watson et al., 2010c).

The hairs on the legs of the cranefly and water strider have a very similar tilted arrangement and alignment of the hair grooves. Anisotropic wetting is reported on the water strider leg as the water contact line has a higher mobility when advancing towards the tip of the leg (Andersen and Cheng, 2005). A similar wetting action may be possible on the cranefly leg and wing, with the finer diagonal grooves further enhancing anisotropic mobility. Also, the similarity between the fine structure of the cranefly smaller wing hairs and water strider leg hairs (Watson et al., 2010a) suggests that droplets may roll off more easily along the direction of patterning.

CONCLUSION

Enhanced by various hair arrangements and their grooves, the low adhesive and wetting properties of the cranefly cuticle allow the insect to interact with a variety of environmental surfaces and conditions where the insect can be immobilized. These findings may contribute to the next generation of bio-inspired materials and devices for the control of interactions at solid–liquid interfaces on macro- and micro-/nano-scales (e.g. the next generation of bio-inspired materials, the design of future robotic insects where weight constraints and surface feature durability are important considerations). Our results support an earlier hypothesis that suggested structures on this length scale (micro-/nano-grooves) found on water striders can resist water adhesion (Watson et al., 2010a).

LIST OF ABBREVIATIONS

AFM	atomic force microscope
CA	contact angle
F–d	force *versus* distance
f_{SL}	fraction of the solid–water interface
k_N	normal spring constant
PDMS	polydimethylsiloxane
R_f	roughness factor
SEM	scanning electron microscope
γ_{LV}	liquid–vapour interfacial energies/tensions
γ_{SL}	solid–liquid interfacial energies/tensions
γ_{SV}	solid–vapour interfacial energies/tensions
θ	CA formed with a smooth surface
θ_C	CA formed with a rough surface

REFERENCES

Adamson, A. W. (1990). *Physical Chemistry of Surfaces*. New York: John Wiley & Sons.

Andersen, N. M. and Cheng, L. (2005). The marine insect Halobates (Heteroptera: Gerridae): biology, adaptations, distribution, and phylogeny. In *Oceanography and Marine Biology: An Annual Review*, Vol. 42 (ed. R. N. Gibson, R. J. A. Atkinson and J. D. M. Gordon), pp. 119-179. Boca Raton, FL: CRC Press-Taylor & Francis (Group).

Bhushan, B. and Jung, Y. C. (2008). Wetting, adhesion and friction of superhydrophobic and hydrophilic leaves and fabricated micro/nanopatterned surfaces. *J. Phys. Condens. Matter* **20**, 225010-225033.

Burton, Z. and Bhushan, B. (2005). Hydrophobicity, adhesion, and friction properties of nanopatterned polymers and scale dependence for micro- and nanoelectromechanical systems. *Nano Lett.* **5**, 1607-1613.

Bush, J. W. M., Hu, D. L. and Prakash, M. (2007). The integument of water-walking arthropods: form and function. In *Advances in Insect Physiology: Insect Mechanics and Control*, Vol. 34 (ed. J. Casas and S. Simpson), pp. 117-192. San Diego, CA: Elsevier Academic Press Inc.

Cassie, A. B. D. and Baxter, S. (1944). Wettability of porous surfaces. *Trans. Faraday Soc.* **40**, 546-551.

Cheng, L. (1973). Marine and freshwater skaters: differences in surface fine structures. *Nature* **242**, 132-133.

Chiou, N. R., Lui, C. M., Guan, J. J., Lee, L. J. and Epstein, A. J. (2007). Growth and alignment of polyaniline nanofibres with superhydrophobic, superhydrophilic and other properties. *Nat. Nanotechnol.* **2**, 354-357.

Cleveland, J. P., Manne, S., Bocek, D. and Hansma, P. K. (1993). A nondestructive method for determining the spring constant of cantilevers for scanning force microscopy. *Rev. Sci. Instrum.* **64**, 403-405.

de Gennes, P. G. (1985). Wetting: statics and dynamics. *Rev. Mod. Phys.* **57**, 827.

Extrand, C. W. (2006). Designing for optimum liquid repellency. *Langmuir* **22**, 1711-1714.

Fowkes, F. M. (ed.) (1964). Dispersion force contributions to surface and interfacial tensions, contact angles, and heats of immersion. In *Contact Angle, Wettability, and Adhesion*, Vol. 43, pp. 99-111. Washington, DC: American Chemical Society.

Gibson, C. T., Watson, G. S. and Myhra, S. (1996). Determination of the spring constants of probes for force microscopy/spectroscopy. *Nanotechnology* **7**, 259-262.

Holdgate, M. W. (1955). The wetting of insect cuticles by water. *J. Exp. Biol.* **32**, 591-617.

Holloway, P. J. (1970). Surface factors affecting the wetting of leaves. *Pestic. Sci.* **1**, 156-163.

Lafuma, A. and Quere, D. (2003). Superhydrophobic states. *Nat. Mater.* **2**, 457-460.

Lau, K. K. S., Bico, J., Teo, K. B. K., Chhowalla, M., Amaratunga, G. A. J., Milne, W. I., McKinley, G. H. and Gleason, K. K. (2003). Superhydrophobic carbon nanotube forests. *Nano Lett.* **3**, 1701-1705.

Ma, M. L. and Hill, R. M. (2006). Superhydrophobic surfaces. *Curr. Opin. Colloid Interface Sci.* **11**, 193-202.

Martines, E., Seunarine, K., Morgan, H., Gadegaard, N., Wilkinson, C. D. W. and Riehle, M. O. (2005). Superhydrophobicity and superhydrophilicity of regular nanopatterns. *Nano Lett.* **5**, 2097-2103.

Nosonovsky, M. and Bhushan, B. (2007). Hierarchical roughness optimization for biomimetic superhydrophobic surfaces. *Ultramicroscopy* **107**, 969-979.

Nosonovsky, M. and Bhushan, B. (2008). Biologically inspired surfaces: Broadening the scope of roughness. *Adv. Funct. Mater.* **18**, 843-855.

Parker, A. R. and Lawrence, C. R. (2001). Water capture by a desert beetle. *Nature* **414**, 33-34.

Perez-Goodwyn, P. (2009). *Anti-Wetting Surfaces in Heteroptera (Insecta): Hairy Solutions to Any Problem*. Berlin: Springer-Verlag.

Sun, T. L., Feng, L., Gao, X. F. and Jiang, L. (2005). Bioinspired surfaces with special wettability. *Acc. Chem. Res.* **38**, 644-652.

Wang, R., Hashimoto, K., Fujishima, A., Chikuni, M., Kojima, E., Kitamura, A., Shimohigoshi, M. and Watanabe, T. (1997). Light-induced amphiphilic surfaces. *Nature* **388**, 431-432.

Watson, G. S., Dinte, B. P., Blach, J. A. and Myhra, S. (2002). Demonstration of atomic scale stick-slip events stimulated by the force versus distance mode using atomic force microscopy. *J. Phys. D Appl. Phys.* **35**, 2066-2074.

Watson, G. S., Blach, J. A., Cahill, C., Nicolau, D. V., Pham, D. K., Wright, J. and Myhra, S. (2004a). Interactions of poly(amino acids) in aqueous solution with charged model surfaces – analysis by colloidal probe. *Biosens. Bioelectron.* **19**, 1355-1362.

Watson, G. S., Dinte, B. P., Blach-Watson, J. A. and Myhra, S. (2004b). Friction measurements using force versus distance friction loops in force microscopy. *Appl. Surf. Sci.* **235**, 38-42.

Watson, G. S., Myhra, S., Cribb, B. W. and Watson, J. A. (2008). Putative functions and functlonal efficiency of ordered cuticular nanoarrays on insect wings. *Biophys. J.* **94**, 3352-3360.

Watson, G. S., Cribb, B. W. and Watson, J. A. (2010a). Experimental determination of the efficiency of nanostructuring on non-wetting legs of the water strider. *Acta Biomater.* **6**, 4060-4064.

Watson, G. S., Cribb, B. W. and Watson, J. A. (2010b). How micro/nanoarchitecture facilitates anti-wetting: an elegant hierarchical design on the termite wing. *ACS Nano* **4**, 129-136.

Watson, G. S., Cribb, B. W. and Watson, J. A. (2010c). The role of micro/nano channel structuring in repelling water on cuticle arrays of the lacewing. *J. Struct. Biol.* **171**, 44-51.

Wei, P. J., Shen, Y. X. and Lin, J. F. (2009). Characteristics of water strider legs in hydrodynamic situations. *Langmuir* **25**, 7006-7009.

White, J. H. (1951). Observations on the life history and biology of *Tipula lateralis* Meig. *Ann. Appl. Biol.* **38**, 847-858.

Zhang, F. X. and Low, H. Y. (2007). Anisotropic wettability on imprinted hierarchical structures. *Langmuir* **23**, 7793-7798.